(Py–Py) and pyrene–pyrazoline (Pr–Py) pairs, randomly begin to form nanoparticles such as those in NP1, which cause the emissions from them to overlap to some extent (Figure 3). As DPP nanoparticles grow further, as is the case for NP2(>100 nm), the enhanced Coulombic interaction energies between molecules[5] cause the Pr–Py pairs to form mainly on the surface of the nanoparticles, because of the larger volume of Pr–Py than Py–Py. This hypothesis explains why the emission from Pr–Py CT states at 570 nm is most intense in NP2 and then gradually decreases from NP2 to NP4(Figure 3); as a result of the decrease of the surface-to-volume ratio from NP2 to NP4. When the nanoparticle size increases further into the bulk phase, the Py–Py pair plays a dominant role in the properties of bulk crystals, and only pyrazoline-like emission is observed. The absence of pyrene monomeric emission in DPP bulk crystals may be a result of a low fluorescence quantum yield in bulk crystals as exhibited by the pyrene bulk crystals (as shown in Figure 3).[16] Therefore, the multiple emission of DPP nanoparticles and their evolution as a function of size is caused by the molecular aggregation and surface effects.

In summary, unlike the corresponding monomers and bulk crystals, DPP nanoparticles were found to exhibit a special type of multiple emission, which ranges from near-UV to green, and as a result of the surface effects, is tunable by alteration of both the excitation wavelength and nanoparticle size,. This novel phenomenon is of interest in the tailoring of the properties of optical materials. Thus, organic crystals also possess significant size effects like those of inorganic semiconductors and metals, but with a greater diversity because of a wide variety of organic molecular structures.

Received: August 27, 2001
Revised: October 22, 2001 [Z17800]

[1] M. A. Hinse, P. Guyot-Sionnest, *J. Phys. Chem.* **1996**, *100*, 468.
[2] A. P. Alivisatos, *Science* **1996**, *271*, 933.
[3] E. A. Silinsh, *Organic Molecular Crystals: Their Electronic States*, Springer, Berlin, **1980**.
[4] M. Pope, C. E. Swenberg, *Electronic Processes in Organic Crystals*, Oxford University Press, Oxford, **1982**.
[5] H. Kasai, H. Kamatani, S. Okada, H. Oikawa, H. Matsuda, H. Nakanishi, *Jpn. J. Appl. Phys. Part 2* **1996**, *35*(2B), L221.
[6] H. Kasai, H. Kamatani, Y. Yoshikawa, S. Okada, H. Oikawa, A. Watanabe, O. Itoh, H. Nakanishi, *Chem. Lett.* **1997**, 1181.
[7] H. Nakanishi, H. Katagi, *Supramol. Sci.* **1998**, *5*, 289.
[8] A. Ibanez, S. Maximov, A. Guiu, C. Chaillout, P. L. Baldeck, *Adv. Mater.* **1998**, *10*, 1540.
[9] Y. Z. Shen, D. Jakubczyk, F. M. Xu, J. Swiatkiewicz, P. N. Prasad, B. A. Reinhardt, *Appl. Phys. Lett.* **2000**, *76*, 1.
[10] H. B. Fu, J. N. Yao, *J. Am. Chem. Soc.* **2001**, *123*, 1434.
[11] X. C. Gao, H. Cao, L. Q. Zhang, B. W. Zhang, Y. Cao, C. H. Huang, *J. Mater. Chem.* **1999**, *9*, 1077.
[12] The size distribution of nanoparticles <100 nm is broad. For example, the polydispersity of nanoparticle NP1 of size 65 nm is about 40%.
[13] N. D. Denkov, O. D. Velev, P. A. Kralchevsky, I. B. Ivanov, H. Yoshimura, K. Nagayama, *Nature* **1993**, *361*, 26.
[14] J. O. Morley, V. J. Docherty, D. Pugh, *J. Mol. Electron.* **1989**, *5*, 117.
[15] Z. L. Yan, G. W. Hu, S. K. Wu, *Acta Chim. Sin. (Chinese Ed.)* **1995**, *53*, 227.
[16] A. Inoue, K. Yoshihara, T. Kasuya, S. Nagakura, *Bull. Chem. Soc. Jpn.* **1972**, *45*, 720.
[17] S. G. Schulman, *Fluorescence and Phosphorescence Spectroscopy: Physicochemical Principles and Practice*, Oxford, New York, **1977**.

Template Effects, Asymmetry, and Twinning in Helical Inclusion Compounds**

Mark D. Hollingsworth,* Michael E. Brown, Michael Dudley, Hua Chung, Matthew L. Peterson, and Andrew C. Hillier

Dedicated to Professor J. Michael McBride

Of the achiral substances in our world, only a small fraction are spontaneously resolved into enantiomorphic crystals that can be separated. Spontaneous resolution may occur when the molecular constituents of the crystal adopt chiral or skewed conformations or when molecules adopt chiral arrangements, such as a helices, which act as templates for further growth of the given enantiomorph. Certain inclusion compounds (such as those derived from urea and tri-*o*-thymotide) have received attention because spontaneous resolution of the inclusion compound leads to chiral discrimination between guest enantiomers.[1, 2] For urea inclusion compounds (UICs), in which urea forms helical channels in the presence of long-chain guests,[3] the literature has uniformly treated these materials as either right- or left-handed homochiral objects. In part, this misconception occurs because the typical needle morphology makes it difficult to observe the presence of enantiomorphic domains. Through the combined use of optical microscopy, synchrotron white beam X-ray topography (SWBXT), and crystallography, we demonstrate here the existence of two types of previously unrecognized macroscopic twinning in UICs. This work provides further support for our models of crystal growth[4] and hydrogen-bond topologies in UICs containing bis(methyl ketone)s[5] and provides a rationale for chiral (Brasil) twinning in these materials. This rationale may serve as a model for chiral twinning in other helical materials,[6] especially those with double helices.

Most urea inclusion compounds consist of well-defined host structures in which urea molecules are hydrogen-bonded to form honeycomb networks of nonintersecting hexagonal channels. Within these channels, long-chain guest molecules

[*] Prof. M. D. Hollingsworth, M. E. Brown, Dr. M. L. Peterson
Chemistry Department
Kansas State University
111 Willard Hall, Manhattan, KS 66506 (USA)
Fax: (+1) 785-532-6666
E-mail: mdholl@ksu.edu
Prof. M. Dudley, Dr. H. Chung
Department of Materials Science and Engineering
State University of New York at Stony Brook
Stony Brook, NY 11794 (USA)
Prof. A. C. Hillier
Department of Chemical Engineering
University of Virginia
Charlottesville, VA 22904 (USA)

[**] We thank J. D. Chaney, S. R. Wilson, B. D. Santarsiero, and J. M. McBride for help with this work, and the donors of the Petroleum Research Fund, administered by the American Chemical Society (29932-AC4), the NSF (CHE-0096157 and DMR-9996243), NASA (NAG8-1702), and the Research Corporation for funding. Topography was carried out at the Stony Brook Synchrotron Topography Station, Beamline X-19C at the National Synchrotron Light Source, Brookhaven National Laboratory, which is supported by the U.S. Department of Energy under contract number DE-AC02-98CH10886.

  1433-7851/02/4106-0965 $ 17.50+.50/0

pack within van der Waals contact. Although UICs typically form high-symmetry, incommensurate (nonstoichiometric) structures,[7] we have identified a series of commensurate UICs containing homologous bis(methyl ketone)s.[3–5, 8] For such guests and their congeners, a reliable host–guest hydrogen-bonding motif can be used to control both internal symmetry and external shape of these crystals. In most bis(methyl ketone)/urea crystals that we have studied, urea molecules turn about their twofold axes to form hydrogen bonds with guest molecules in adjacent channels. Using this motif, we have developed a simple geometric model that allows us to use the host:guest stoichiometry, natural length of the guest, and the parity (odd or even) of the guest molecule's chain to restrict the possible host–guest hydrogen-bonding topologies. In the case of 2,12-tridecanedione/urea (**1**/urea), our prediction of the correct polymorphic structure was instrumental in our structure solution and refinement from the X-ray data.

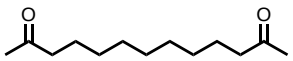

1

A description of helical wheels is given elsewhere,[5] so only the salient features are presented here. Most UICs are chiral objects in which the two intertwined helices are of the same handedness and are related by C_2 axes perpendicular to the channel. Each urea molecule in helix 1 (numbered 1, 2, and so on as one moves down the channel) has a counterpart directly across the channel (at the same z coordinate) in helix 2 (numbered 1′, 2′, and so on). These pairs of molecules (for example, 1 and 1′) lie parallel to each other. If the host:guest stoichiometry is known (or can be predicted), it is a simple matter to write down the relative positions of the urea molecules that are in position to use their *syn* N–H groups to form hydrogen bonds with the guest. For **1**/urea, the natural length of the guest (18.8 Å)[3, 4, 9] predicts a host:guest stoichiometry of 10:1, so the hydrogen-bonding motif requires that the two C=O groups of a given guest molecule are tethered to urea molecules in the first and eleventh positions in the channel (since half of a urea molecule is used at each end of the guest). The helical-wheel diagram shown in Figure 1 represents four possible combinations of host–guest connectivities (1–11, 1–11′, 1′–11, 1′–11′), the first and fourth of which are degenerate. Long arrows in the center of each diagram denote the orientations of the two carbonyl groups in one guest molecule and give a rough idea of the dihedral angle between them.

For this odd-chain guest, whose natural length is slightly longer than the commensurate repeat of 18.36 Å, Figure 1B predicts that a stable structure (with low torsional strain) can be formed. Indeed, the channel axis oscillation photograph indicates a commensurate structure with $3c'_g = 5c'_h$ (urea:guest = 10:1), and the crystals grow as thin {001} plates, as predicted for a commensurate structure in which guests are tethered to the host and offset from guests in adjacent channels by 0 Å.[4] Further support for this structural motif came from atomic force microscopy (AFM), which showed that terraces on the {001} faces are molecularly smooth and offset

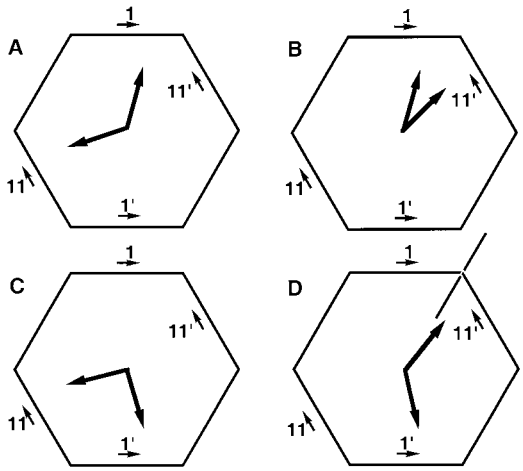

Figure 1. Right-handed helical-wheel diagram showing four possible arrangements for host–guest hydrogen bonding in **1**/urea. (An equivalent diagram can be drawn for a left-handed helix.) The numbered arrows around the periphery of the hexagon refer to the orientations of urea C=O groups. The C_2 axis shared by A and D (which are degenerate) is shown in D. For this odd-chain guest, this simple model correctly predicts topology B (see Figure 4e).

along c by integral multiples of the guest length, with average height of 18.1(5) Å or a multiple thereof (Figure 2). Nevertheless, our early attempts to solve the structure from area detector data proved unsuccessful because of disorder of the guest.

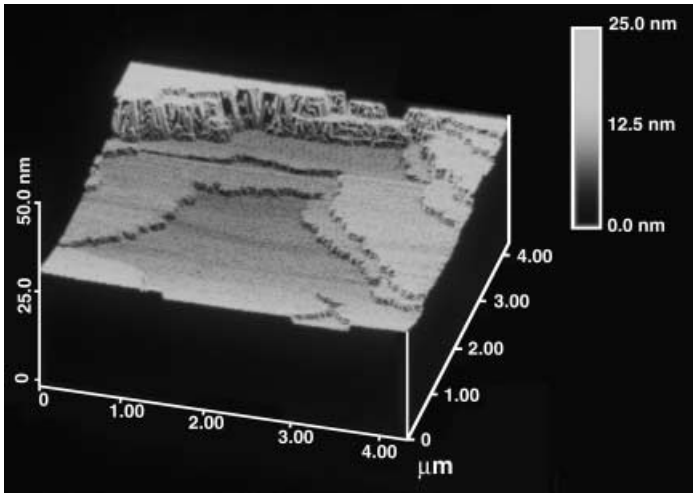

Figure 2. AFM images of the {001} face of **1**/urea recorded in air on a Digital Nanoscope III instrument in tapping mode. The average step height for six different ledges was 18.1(5) Å or a multiple thereof.

For a commensurate structure of **1**/urea with $3c'_g = 5c'_h$ one predicts that guests will be related by threefold (3_1) screw axes along the channels and that the crystals will therefore have uniaxial optical properties (that is, with no ferroelastic distortion in the *ab* plane).[8] Photomicrographs can therefore reveal optical activity, which for most UICs is relatively insensitive to guest identity in the visible region of the spectrum.[2b] Because there were no previous reports of chiral twinning in UICs, we were surprised to find that in **1**/urea and related materials (2-tridecanone/urea, 2,9-decanedione/

  1433-7851/02/4106-0966 $ 17.50+.50/0 *Angew. Chem. Int. Ed.* **2002**, *41*, No. 6

urea,[4] and mixed UICs of 2-undecanone and 6-undecanone), both dextrorotatory and levorotatory domains could be observed (Figure 3a and b). The twin boundaries that separate these domains occur every 60° and are coincident with the {110} faces of the crystal.

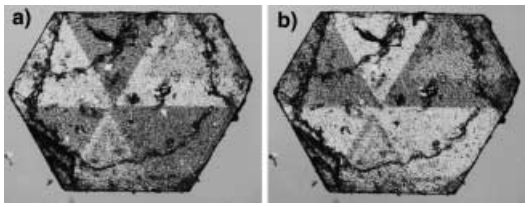

Figure 3. a) Photomicrograph of **1**/urea (0.26 mm thick) with polarized light at 546 nm and the analyzer rotated by +9° from the crossed position (dark = dextrorotatory). b) The same crystal with the analyzer rotated by −9° from the crossed position (dark = levorotatory). In each, the view is down the channel axis.

Because the nature of the twin boundaries in UICs was important for our studies of domain switching in ferroelastic UICs[8] (whose birefringence would mask any chiral twinning), we subjected this crystal to SWBXT at beamline X-19C at the National Synchrotron Light Source. In this technique, the highly collimated white beam provides topographic images with high spatial resolution for each Bragg reflection.[10] The positions and intensities of the resulting images are sensitive to twinning, strain, dislocations, and differences in structure factors for reflections in different domains.[11] After an exposure of 10–15 s, one obtains a Laue image corresponding to the most intense reflections in the diffraction pattern (Figure 4a). For **1**/urea, reflections occur in three separate sets, one of which shows no contrast. The other two sets form complementary images (labeled **d** and **e**) that reveal sectoring *in addition to* the chiral twinning described above (Figure 4b and c) and little or no apparent strain at any of the domain boundaries.

In anticipation of a trigonal structure, we indexed the topograph with a nonprimitive, rhombohedral cell ($a = 55.96$ Å, $\alpha = 14.63°$),[12] and found that in the **d** and **e** reflections, the contrast pattern obeyed the conditions for obverse and reverse settings of a rhombohedral cell ($-h+k+l = 3n$ and $h-k+l = 3n$). These unit cells are related by 180° (or equivalent 60°) rotation about the channel axis.[13] Although this rotational (Dauphiné) twinning[14] was invisible under the microscope, the X-ray topograph could be used as a guide for cleavage of this crystal into eleven fragments. Two complementary fragments [fragment **7**-(+)-**e** (dextrorotatory type **e**) and fragment **2**-(−)-**d** (levorotatory type **d**)] were used for X-ray data collection at −75 °C (see arrows in Figure 4b and c).

Structure solution and refinement revealed that the apparent rhombohedral symmetry was only approximate, and that the structures could be solved in the trigonal space groups $P3_112$ and $P3_212$. Because there are no heavy atoms in these structures, the absolute structures could not be determined unambiguously with either Flack or Bijvoet methods,[15] but the favored assignments (Figure 4d and e) agree with Schlenk's model-based correlation of positive optical rotation

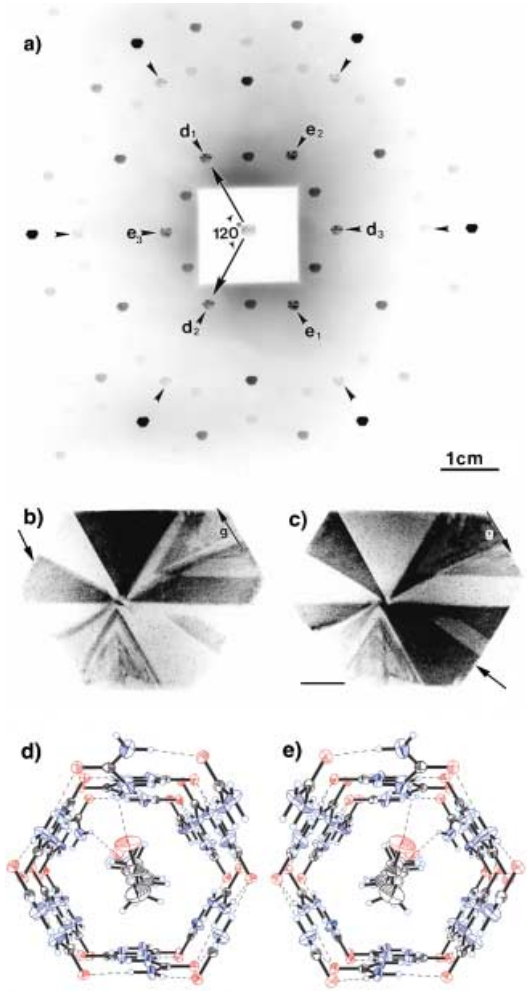

Figure 4. a) SWBXT Laue image of **1**/urea held with its {001} face perpendicular to the X-ray beam. Note complementary contrast in reflections labeled **d** and **e**. b) SWBXT of $\mathbf{d_1}$ reflection for **1**/urea (***g*** vector shown in upper right). Arrow on left denotes levorotatory region (**2**-(−)-**d**) used for X-ray crystal structure shown in Figure 4d (see text). c) SWBXT of $\mathbf{e_1}$ reflection for **1**/urea (***g*** vector shown in upper right). Arrow on right denotes dextrorotatory region (**7**-(+)-**e**) used for X-ray crystal structure shown in Figure 4e. Scale bar: 400 μm. d) and e) ORTEP diagrams (30% ellipsoids) showing $P3_212$ crystal structure of levorotatory fragment shown in Figure 4b (d) and $P3_112$ crystal structure of dextrorotatory fragment shown in Figure 4c (e). The absolute configurations are not proven.

with the right-handed (3_1) sense of the urea helix.[2b] Nevertheless, the structures[16] confirm that in the presence of host–guest hydrogen bonding, the helical-wheel method correctly predicts the observed polymorph (cf. Figures 1B and 4e).

Facet indexing and correlation with the overall crystal morphology showed that the **d** and **e** domains are related to each other by 60° rotation about the channel axis. (For fragment **2**-(−)-**d**, which was contaminated by a small amount of the adjacent type **e** domain, the largest peak in the difference Fourier map assumed the position of an oxygen atom in a guest carbonyl group rotated 58° about the channel axis.) This macroscopic rotational twinning is established during crystal growth, persists over a period of years, and is remarkable given the dynamic nature of guests in other UICs[17] and the lack of ferroelastic distortion in **1**/urea. (SWBXT of the upper right third of this crystal, which was

  1433-7851/02/4106-0967 $ 17.50+.50/0

held between −20 and 20 °C for two years after the initial topograph, showed no noticeable degradation in the Dauphiné twin boundaries.)

Although chiral twinning is counterintuitive in a strongly hydrogen-bonded helical system, in which templated growth predominates, clues to the twinning mechanism in **1**/urea come from our recent structures of a series of centrosymmetric UICs.[18] For $Br(CH_2)_6Br$/urea and congeners (space group $P2_1/n$, *b* unique), the *n*-glide provides a convenient mechanism by which the structures on either side of certain (001)-type channel walls are related by mirror symmetry. In $Br(CH_2)_6Br$/urea, the *n*-glide generates a looplike topology of hydrogen bonds in which certain rows of urea molecules lying closest to the (001) plane are translated along the channel relative to their counterparts in helical structures. From a diagram based on our helical-wheel formalism, it is possible to show that the loop topology in $Br(CH_2)_6Br$/urea can serve as a template for the formation of enantiomorphic helices above and below the (001) plane (Figure 5). (No other primitive planes in the $Br(CH_2)_6Br$/urea structure can directly template

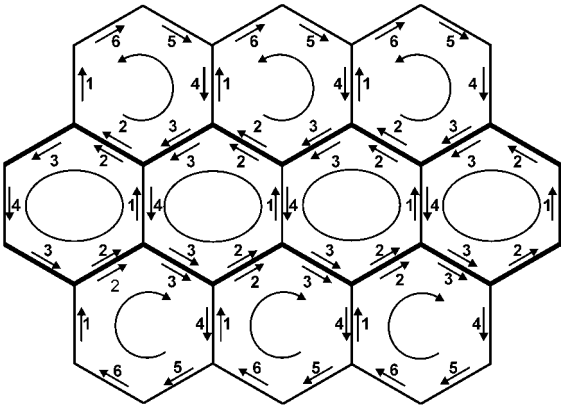

Figure 5. Modified helical-wheel diagram showing how the stacked loop structure of a centrosymmetric UIC (such as $Br(CH_2)_6Br$/urea) can serve as a template for the formation of left- and right-handed helices above and below the (001) plane. Arrows in the middle row of channels correspond to C=O axes for urea molecules in the $P2_1/n$ structure found in numerous $X(CH_2)_6X$/urea inclusion compounds. The numbers correspond to the relative positions along the channel axis of those urea molecules. At the bottom of this centrosymmetric row, urea molecules 2 and 3 template the formation of a right-handed helix, in which the sequence 1, 2, 3, 4, 5, 6 leads in a clockwise sense away from the observer (down the channel). At the top, urea molecules 2 and 3 template the formation of a left-handed helix (counterclockwise from 1 through 6). These right- and left-handed helices correspond to the unprimed and primed helices described above in the helical-wheel formalism.

both right- and left-handed helices.) Although the precise structure of the chiral twin boundaries is not available from SWBXT of **1**/urea, support for this twinning mechanism comes from the structural correspondence between the {001} planes in $Br(CH_2)_6Br$/urea and the {110} planes of **1**/urea, which exhibit chiral twinning.[18]

Athough **1**/urea is not ferroelastic, these results illuminate our studies of domain switching in ferroelastic crystals such as 2,10-undecanedione/urea, in which domain reorientation occurs under applied external anisotropic stress.[8] Because the present work shows that chiral twinning may occur in helical urea systems, and that the most likely topology at this type of domain boundary is nonhelical, we anticipate that ferroelastic UICs containing such twin boundaries will have high barriers to domain wall motion.[19] With the recent emergence of optical techniques for measuring chirality in biaxial crystals,[20] identification of Brasil-type domain walls may soon be possible.

Experimental Section

1/urea: A solution of 2,12-tridecanedione (0.301 g, 1.42 mmol, prepared by literature methods[21]), urea (0.857 g, 14.3 mmol, Baker AR) and MeOH (7.0 mL, Mallinckrodt) was allowed to evaporate at RT. After one day, thin plates (0.331 g) were collected. M.p. 134.5–135 °C, uncorrected; ^{1}H NMR (400 MHz, [D$_6$]DMSO): $\delta = 5.41$ (s, urea), 2.38 (t, $^3J(H,H) = 7.4$ Hz), 2.04 (s), 1.41 (m), 1.20 (m), urea:guest (10.3:1); IR (Nujol): $\tilde{\nu} = 1717$ cm^{-1}.

Received: September 24, 2001 [Z17957]

[1] a) R. Arad-Yellin, B. S. Green, M. Knossow, G. Tsoucaris in *Inclusion Compounds*, *Vol. 3* (Eds.: J. L. Atwood, J. E. Davies, D. D. MacNicol), Academic Press, Orlando, **1984**, pp. 263–295; b) R. Gerdil in *Comprehensive Supramolecular Chemistry*, *Vol. 6* (Eds.: J. L. Atwood, J. E. D. Davies, D. D. MacNicol, F. Vögtle), Elsevier Science, Oxford, **1996**, pp. 177–237.

[2] a) W. Schlenk, Jr., *Angew. Chem.* **1960**, *72*, 845–849; b) W. Schlenk, Jr., *Chem. Ber.* **1968**, *101*, 2445–2449; c) W. Schlenk, Jr., *Justus Liebigs Ann. Chem.* **1973**, 1145–1155; W. Schlenk, Jr., *Justus Liebigs Ann. Chem.* **1973**, 1156–1178; W. Schlenk, Jr., *Justus Liebigs Ann. Chem.* **1973**, 1179–1194; W. Schlenk, Jr., *Justus Liebigs Ann. Chem.* **1973**, 1195–1209.

[3] M. D. Hollingsworth, K. D. M. Harris in *Comprehensive Supramolecular Chemistry*, *Vol. 6* (Eds.: J. L. Atwood, J. E. D. Davies, D. D. MacNicol, F. Vögtle), Elsevier Science, Oxford, **1996**, pp. 239–280.

[4] M. D. Hollingsworth, M. E. Brown, A. C. Hillier, B. D. Santarsiero, J. D. Chaney, *Science* **1996**, *273*, 1355–1359.

[5] M. E. Brown, J. D. Chaney, B. D. Santarsiero, M. D. Hollingsworth, *Chem. Mater.* **1996**, *8*, 1588–1591.

[6] a) B. S. Green, M. Knossow, *Science* **1981**, *214*, 795–797; b) S. Furberg, O. Hassel, *Acta Chem. Scand.* **1950**, *4*, 1020–1023; c) R. J. Davey, S. N. Black, L. J. Williams, D. McEwan, D. E. Sadler, *J. Cryst. Growth* **1990**, *102*, 97–102; d) G. A. Potter, C. Garcia, R. McCague, B. Adger, A. Collet, *Angew. Chem.* **1996**, *108*, 1780–1782; *Angew. Chem. Int. Ed. Engl.* **1996**, *35*, 1666–1668; e) M. Berfeld, D. Zbaida, L. Leiserowitz, M. Lahav, *Adv. Mater.* **1999**, *11*, 328–331; f) D. Zbaida, M. Lahav, K. Drauz, G. Knaup, M. Kottenhahn, *Tetrahedron* **2000**, *56*, 6645–6649.

[7] K. D. M. Harris, J. M. Thomas, *J. Chem. Soc. Faraday Trans.* **1990**, *86*, 2985–2996.

[8] M. E. Brown, M. D. Hollingsworth, *Nature* **1995**, *376*, 323–327.

[9] H. U. Lenné, H. C. Mez, W. Schlenk, Jr., *Justus Liebigs Ann. Chem.* **1970**, *732*, 70–96.

[10] a) J. Miltat, M. Dudley in *Applications of Synchrotron Radiation* (Ed.: R. A. Catlow), Blackie Publishers, London, **1990**, pp. 65–99; b) M. Dudley, *Encyclopedia of Applied Physics*, *Vol. 21*, Wiley-VCH, Weinheim, **1997**, pp. 533–547.

[11] H. Chung, M. Dudley, M. E. Brown, M. D. Hollingsworth, *Mol. Cryst. Liq. Cryst.* **1996**, *276*, 203–212.

[12] A primitive rhombohedral cell with cell constants $a = 19.05$ Å and $\alpha = 24.94°$ does not accommodate the threefold screw axis predicted for this guest.

[13] See K. D. M. Harris, S. P. Smart, M. D. Hollingsworth, *J. Chem. Soc. Faraday Trans.* **1991**, *87*, 3423–3429 for a related system.

[14] J. Tullis, *Science* **1970**, *168*, 1342–1344.

[15] a) H. D. Flack, *Acta Crystallogr. Sect. A* **1983** *39*, 876–881; b) J. M. Bijvoet, A. F. Peerdeman, A. J. van Bommel, *Nature* **1951**, *168*, 271–272.

  1433-7851/02/4106-0968 $ 17.50+.50/0

[16] Crystal data for (+)-**1**/urea (space group $P3_112$): $a=b=8.1660(10)$, $c=55.2445(13)$ Å, $V=3190.8(1)$ Å^3 at 198 K; $R_1=0.085$, $wR_2=0.095$, GOF 1.747 (based on F^2), 5081 observed reflections with $I\geq 2.00\sigma(I)$, 252 parameters, Flack x parameter (esd) $=-1.38$ (1.66). Crystal data for (−)-**1**/urea (space group $P3_212$): $a=b=8.1670(10)$, $c=55.2166(12)$ Å, $V=3189.5(1)$ Å^3 at 198 K; $R_1=0.095$, $wR_2=0.069$, GOF 2.513 (all reflections, based on F^2), 3670 observed reflections with $I\geq 2.00\sigma(I)$, 252 parameters, Flack x parameter (esd) $=-1.55$ (1.77). (Other trigonal UICs, such as 2,9-decanedione/urea[4] give similar results and errors. Extensive efforts to prepare heavy atom analogues amenable to Bijvoet analysis are underway.) CCDC-171162 ((−)-**1**/urea) and CCDC-171163 ((+)-**1**/urea) contain the supplementary crystallographic data for this paper. These data can be obtained free of charge via www.ccdc.cam.ac.uk/conts/retrieving.html (or from the Cambridge Crystallographic Data Centre, 12, Union Road, Cambridge CB2 1EZ, UK; fax: (+44) 1223-336-033; or deposit@ccdc.cam.ac.uk).

[17] U. Werner-Zwanziger, M. E. Brown, J. D. Chaney, E. J. Still, M. D. Hollingsworth, *Appl. Magn. Reson.* **1999**, *17*, 265–281.

[18] M. D. Hollingsworth, U. Werner-Zwanziger, M. E. Brown, J. D. Chaney, J. C. Huffman, K. D. M. Harris, S. P. Smart, *J. Am. Chem. Soc.* **1999**, *121*, 9732–9733.

[19] M. D. Hollingsworth, M. L. Peterson, K. L. Pate, B. D. Dinkelmeyer, M. E. Brown, *J. Am. Chem. Soc.* **2002**, *124*, in press.

[20] W. Kaminsky, A. M. Glazer, *Z. Kristallogr.* **1997**, *212*, 283–296.

[21] G. H. Posner, C. E. Whitten, P. E. McFarland, *J. Am. Chem. Soc.* **1972**, *94*, 5106–5108.

Structural Analysis of C_{60} Trimers by Direct Observation with Scanning Tunneling Microscopy **

Masashi Kunitake,* Shinobu Uemura, Osamu Ito, Koichi Fujiwara, Yasujiro Murata, and Koichi Komatsu*

All-carbon fullerene oligomers and polymers have attracted considerable interest from a wide range of scientific and technological view points.[1] The formation, structure, and characteristics of fullerene oligomers, such as dimers and trimers, and fullerene polymers are of particular interest because of their potential usefulness as molecular devices, and in the fields of optoelectronics and nanotechnology. These materials have been prepared under photochemical[2] or high-pressure/high-temperature conditions,[3] or by the action of alkali metals upon fullerenes.[4] Recently, it was found that the solid-state mechanochemical reaction of C_{60} with potassium salts such as KCN, KOAc, and K_2CO_3, with highly reducing metals, or with solid aromatic amines under "high-speed vibration milling (HSVM)" conditions, can successfully produce the fullerene dimer, C_{120}.[5, 6] Furthermore, the trimers (C_{180}), which include a variety of structural isomers, were also found to be formed by this reaction.[7]

When C_{60} was treated with 4-aminopyridine under HSVM conditions, analysis of the reaction mixture with high-pressure liquid chromatography (HPLC) using a Cosmosil 5PBB column and eluting with *o*-dichlorobenzene (*o*-DCB) showed two small peaks (fractions A and B) corresponding to the trimer (C_{180}). These peaks appeared after the major peaks for C_{60} and the dimer (C_{120}). Upon evaporation of the solvent, the material giving rise to the C_{180} peaks amounted to 4% yield based on C_{60}. Further analysis and separation using different HPLC conditions with a Cosmosil Buckyprep column and eluting with toluene revealed that fraction A consisted of at least three isomers (A1, A2,[16] and A3), while fraction B was a single component (Figure 1). The identity of C_{180} was established by solution-phase cyanation and observation of the peak arising from the $C_{180}(CN)^-$ ion by atmospheric pressure chemical ionization (APCI) mass spectral analysis (negative ion mode). APCI mass analysis of the C_{180} itself exhibited only the fragment peak of C_{60}.[7]

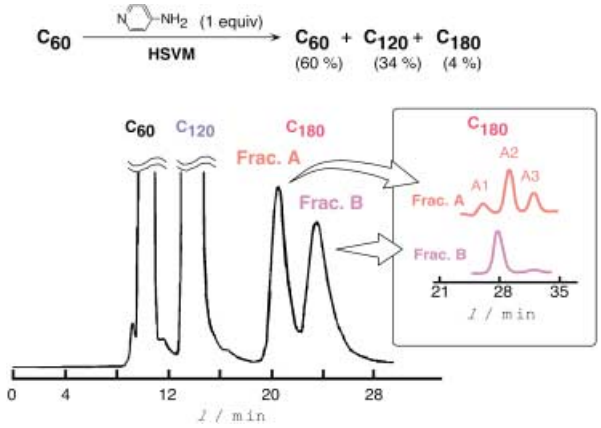

Figure 1. Elution traces for HPLC separation of C_{180} isomers, with UV detection at 326 nm. Left: Cosmosil 5PBB column eluting with *o*-DCB, and right (inset): Cosmosil Buckyprep column eluting with toluene.

Unfortunately, the extremely low solubility of C_{180} in ordinary solvents did not allow the chemical structure to be determined by ^{13}C NMR spectroscopy. Such low solubility also made it difficult to prepare single-crystal samples of C_{180} for X-ray diffraction analysis. In the present study, however, we successfully achieved structural identifications of the C_{180} isomers by direct visualization using scanning tunneling microscopy (STM).

[*] Prof. Dr. M. Kunitake, Dr. S. Uemura
Department of Applied Chemistry & Biochemistry
Faculty of Engineering, Kumamoto University
Kurokami, Kumamoto 860-8555 (Japan)
Fax: (+81) 96-342-3673
E-mail: kunitake@chem.kumamoto-u.ac.jp
Prof. Dr. K. Komatsu, K. Fujiwara, Dr. Y. Murata
Institute for Chemical Research
Kyoto University
Uji, Kyoto 611-0011 (Japan)
Fax: (+81) 774-38-3178
E-mail: komatsu@scl.kyoto-u.ac.jp
Prof. Dr. O. Ito
Institute of Multidisciplinary Research for Advanced Materials
Tohoku University,Katahira, Sendai, 980-8577 (Japan)

[**] This work was supported in part by Grants-in-Aids for Scientific Research from the Ministry of Education, Culture, Sports, Science, and Technology, Japan and the CREST- JST, Japan.

  1433-7851/02/4106-0969 $ 17.50+.50/0